The Role of Sea Ice in 2 × CO_2 Climate Model Sensitivity. Part I: The Total Influence of Sea Ice Thickness and Extent

D. RIND

Goddard Space Flight Center, Institute for Space Studies, New York, New York

R. HEALY

Lamont-Doherty Earth Observatory and Department of Geological Sciences, Columbia University, Palisades, New York

C. PARKINSON

Goddard Space Flight Center, Oceans and Ice Branch, Greenbelt, Maryland

D. MARTINSON

Lamont-Doherty Earth Observatory and Department of Geological Sciences, Columbia University, Palisades, New York

(Manuscript received 11 January 1994, in final form 3 August 1994)

ABSTRACT

As a first step in investigating the effects of sea ice changes on the climate sensitivity to doubled atmospheric CO_2, the authors use a standard simple sea ice model while varying the sea ice distributions and thicknesses in the control run. Thinner ice amplifies the atmospheric temperature sensitivity in these experiments by about 15% (to a warming of 4.8°C), because it is easier for the thinner ice to be removed as the climate warms. Thus, its impact on sensitivity is similar to that of greater sea ice extent in the control run, which provides more opportunity for sea ice reduction. An experiment with sea ice not allowed to change between the control and doubled CO_2 simulations illustrates that the total effect of sea ice on surface air temperature changes, including cloud cover and water vapor feedbacks that arise in response to sea ice variations, amounts to 37% of the temperature sensitivity to the CO_2 doubling, accounting for 1.56°C of the 4.17°C global warming. This is about four times larger than the sea ice impact when no feedbacks are allowed. The different experiments produce a range of results for southern high latitudes with the hydrologic budget over Antarctica implying sea level increases of varying magnitude or no change. These results highlight the importance of properly constraining the sea ice response to climate perturbations, necessitating the use of more realistic sea ice and ocean models.

1. Introduction

This is the first paper in a series presenting results of ongoing research to explore the influence of sea ice on climate sensitivity as simulated in a general circulation model. Of the different features contributing to climate sensitivity, the ice–albedo feedback is thought to be one of the more certain; as climate warms, the sea ice and snow cover should eventually decrease, lowering the surface albedo, increasing the solar radiation absorbed at the surface, and thus providing a positive feedback to the initial warming. Certain questions have been raised about some aspects of this scenario; for example, perhaps with increased temperatures and thus greater evaporation and increased atmospheric water-holding capacity, snow cover might actually expand at high latitudes where the temperature would still be below freezing in the winter (Miller and Vernal 1992). Observations of the relationship between temperatures and snow cover during the past decade fail to verify this hypothesis (Robinson et al. 1990), and most GCM results consistently indicate reduced snow cover for warmer climates (Cess et al. 1991), but it is still conceivable, especially for Antarctica, where crude estimates imply snow cover has been increasing along with increasing global temperatures during the last several decades (e.g., Morgan et al. 1991; Peel 1992). Sea ice cover changes will undoubtedly affect the availability of moisture and, thus, snow cover response at high latitudes; thus far, no simple relationships have been established between sea ice extent and temperature trends (Houghton et al. 1992).

Sea ice formation depends on the sea surface temperature and heat flux, and in a warming climate with warmer surface waters, sea ice reduction seems inevitable unless shifts in ocean circulation result in less

Corresponding author address: Dr. David Rind, NASA/GISS, 2880 Broadway, New York, NY 10025.

warm water transport into the polar regions. This view of the sea ice response has generally been accepted, at least qualitatively. In GCM simulations of the $2 \times CO_2$ climate, the sea ice response has been large; for example, in the Goddard Institute for Space Studies (GISS) GCM, sea ice cover decreased from 4.1% of the globe in the current climate control run to 2.3% in the case of a 4.2°C warming. In the Southern Hemisphere the annual average sea ice was reduced by 60%, while in the Northern Hemisphere it was reduced by 28% (Hansen et al. 1984).

The effect of sea ice on model simulations is somewhat larger in a cooling climate than in a warming climate. With the GISS model, a 2% increase in the solar irradiance raises the surface air temperature some 4°C (Hansen et al. 1984), while a 2% reduction causes cooling close to 5.8°C (Rind and Overpeck 1994). The greater magnitude in the cooling experiment is associated primarily with a greater geographic area for sea ice growth, and positive albedo feedback, than is available for sea ice reduction (Pollack et al. 1993). One theory of the initiation of ice ages proposes that changes in Arctic sea ice due to orbital variation influences on solar radiation reduce North Atlantic Deep Water (NADW) production, which in turn leads to an increase in sea ice near Antarctica. The sea ice changes would thus provide amplification of the relatively weak orbital forcing, producing the initial cooling for ice ages (Imbrie et al. 1992).

The magnitude of the sea ice contribution to climatic warming in the $2 \times CO_2$ climate has been estimated in a variety of ways, ranging from analysis of the direct impact of sea ice using 1D radiative–convective models with the annual, global average changes produced in a 3D GCM (Hansen et al. 1984), to analysis of the full impact of sea ice through experiments in which the sea ice is not allowed to change as the climate warms (Ingram et al. 1989). In the latter study, it was clearly shown that the magnitude of the sea ice feedback varies with the method of computation. We will repeat several of the calculations here to establish a baseline response for the subsequent experiments.

The variation in the amount of sea ice in different model control runs is thought to be one of the important ingredients responsible for different climate sensitivities in models. Specifically, if the control run has too much sea ice, it has more to lose in the $2 \times CO_2$ experiments, amplifying the model response, and producing greater warming (e.g., Spelman and Manabe 1984). GCM experiments with ocean slab mixed layers and no ocean dynamics that do not use the so-called "q flux" correction (specified ocean heat convergences) often suffer from this problem, which also then exaggerates the high-latitude/low-latitude temperature response (e.g., Spelman and Manabe 1994). However, incorporating the q flux in such a manner as to produce the "observed" sea ice is no easy task. The heat convergence into a grid box with sea ice can be put into the water under the ice, warming this water, and causing melting and, thus, thinning of the ice by heat transfer from the water below via heat conduction—"heat conduction from below." It can be put directly into the ice bottom, causing thinning in a more efficient manner—"heat insertion from below"; or it can be put laterally into the ice to cause horizontal contraction (opening up of the leads)—"heat insertion from the sides." Each approach produces a somewhat different sea ice response and, hence, a different global sensitivity to $2 \times CO_2$. In Hansen et al. (1984), the "heat conduction from below" approach left the control run with 20% too much sea ice and a sensitivity to $2 \times CO_2$ of 4.8°C; an experiment using "heat insertion from below" and "heat insertion from the sides" (50% each) produced 15% too little sea ice and a 4.2°C sensitivity.

Another problem concerns the observed sea ice that the control run is attempting to reproduce. Sea ice observations from Alexander and Mobley (1974), Walsh and Johnson (1979), and satellite observations (e.g., Zwally et al. 1983; Parkinson et al. 1987; Gloersen et al. 1992) can provide approximate geographical variations in sea ice extent; however, they do not indicate the sea ice thicknesses, which have been measured only sporadically in situ. Models will generally use "reasonable" sea ice thicknesses in their control run prescriptions, and these values are then employed for q flux calculations. However, as indicated above, it is not easy to control the sea ice with the q flux procedure, and this holds true for sea ice thickness as well as sea ice extent. If no q flux is used, it would be even harder to bound sea ice thicknesses.

In regions with thick sea ice, an overestimation in models probably will not affect climate sensitivity, since there should be little change in insulating capability above a certain sea ice thickness. However, there is no guarantee that sea ice thickness is not being overestimated in regions of thin or seasonal sea ice, as will be shown below for the GISS standard $2 \times CO_2$ run. Some modelers tend not to show sea ice thicknesses for their control runs (perhaps because the intent is to compare the control run with observations and there are no standard sea ice thickness datasets), so the pervasiveness of the problem is hard to estimate. Our experience has been that if the experiment is run long enough, then unless artificially limited, sea ice thickness will become extreme in some grid points due to the simplicity of the sea ice parameterization used. In the study reported here, we will indicate the influence that the use of more realistic sea ice concentrations and thicknesses in the control run has on the simulated climate sensitivity.

As the response of sea ice depends upon the reaction of the surface water temperatures and surface fluxes, any processes that affect the ocean will affect the sea ice. Mixed layer models run for $2 \times CO_2$ experiments generally do not allow for a change in ocean heat transports (the q flux is the same in both the experiment

and control runs). Rind and Chandler (1991) show that an increase in poleward ocean heat transports of just 15% globally (although greater locally at high latitudes) is sufficient in the GISS GCM to remove all sea ice. As a by-product of the experiments performed here, we will show how changes in ocean heat transports can significantly affect sea ice thickness and, thus, climate sensitivity.

Finally, all the models used so far for $2 \times CO_2$ experiments with mixed layer ocean simulations have employed simplistic sea ice schemes, generally involving only simple thermodynamics, which allow for several important positive feedbacks but tend to minimize the negative feedbacks. The actual sea ice response is much more complicated, with important sea ice advection effects, and negative feedbacks associated with ocean–sea ice interaction (e.g., overturning) in the Southern Ocean. Proper simulation of the latter process requires much finer vertical resolution than is normal [e.g., Martinson (1993) uses 1-m vertical resolution in his 1D sea ice model], so it is not likely to be accurate even in the current coupled atmosphere–ocean dynamics models. Without better sea ice parameterizations (including the effects of finer vertical resolution), the sea ice contribution to climate sensitivity cannot be fully understood. It may well be very different on the longer timescales when NADW production changes can propagate to the Southern Ocean than for transient or even $2 \times CO_2$ climate changes. The impact of increasingly more realistic sea ice and ocean models on climate and regional sensitivity are the subjects of the second and third papers in this series.

2. Sea ice in the old control and $2 \times CO_2$ experiments

The model used for the experiments performed in this paper is the GCM described by Hansen et al. (1983, 1984). First, a "specified ocean" current climate simulation is made to calculate the required q flux values; then the "varying ocean" control and experiment are run using the calculated q flux. The control and the experiments were each integrated for 35 yr; equilibrium was established by year 25 and results were obtained for years 26–35.

The sea ice cover in the specified ocean present day climate simulation comes from Walsh and Johnson (1979) for the Northern Hemisphere and Alexander and Mobley (1974) for the Southern Hemisphere. As will be shown below, the zonally averaged spatial distribution of these datasets is not much different from that generated using passive-microwave satellite data.

Neither of these two datasets supplies sea ice thickness. Hansen et al. (1983) calculated the sea ice thickness (z_{ice}) for the specified ocean from the fractional ice coverage ($1 - f_0$), where f_0 is the fraction of open ocean, with the formula

$$z_{ice}(m) = 1 + (1 - f_0) z_{max}. \quad (1)$$

Here z_{max} is $n^{1/2}$, where n is the number of months with at least some ice in the gridbox, except $z_{max} = 4$ if $n = 12$. This sea ice thickness parameterization embodied the concept that sea ice would be thicker the more continuously it was present. We shall show below that it overestimated sea ice thickness, especially in the Southern Hemisphere.

The fraction of open water is based on a climatological dataset (e.g., Orvig 1970), except it is limited to

$$f_0 \geq 0.1 / z_{ice} \quad (2)$$

to represent the effect of leads. Thus, for a sea ice thickness of 1 m, the leads are at least 10% of the grid box (the model allows for fractional amounts of sea ice and open ocean in each grid), for 2-m thickness, the leads are at least 5%, etc. Since the sea ice was generally several meters thick, the leads were generally substantially less than 10%.

These formulations were for the specified ocean current climate simulation. Their relevance to the experiments here, in which sea ice thickness and the fraction of open ocean were calculated directly, is that the specified run was used to calculate the q fluxes for the varying ocean (Hansen et al. 1984).

Several additional model parameterizations discussed by Hansen et al. (1983) are relevant to the following discussion. The sea ice albedo in the model is approximated as 0.55 in the visible and 0.3 in the infrared, leading to a spectrally weighted sea ice albedo of 0.45. Snow falling on the ice is made to accumulate as snow until it reaches a depth of 10 cm (equivalent water). Then 1 cm is added to the lower layer as ice. The specified snow albedo varies from 0.85 to 0.5 depending on age (Hansen et al. 1983).

The standard GISS model control and $2 \times CO_2$ experiments used a specified q flux with "heat insertion from below and from the sides" (rather than input to the water beneath the ice) producing both horizontal shrinking and vertical thinning with the energy partitioned equally to the two effects. The annual average zonal sea ice concentrations produced by this approach are shown in Fig. 1 as the "old control sea ice." When CO_2 was doubled it resulted in a 4.2°C warming and a relative sea ice reduction of 44% (from 4.1% absolute to 2.3%). These runs will be referred to as the "old control run" and "old $2 \times CO_2$," respectively.

An alternate control run was made in which the q flux melted sea ice by warming the water below and allowing heat conduction through the ice ("heat conduction from below"). This approach resulted in greater sea ice concentrations, especially in the Southern Hemisphere (Fig. 1) (henceforth "alternate old control" and "alternate old $2 \times CO_2$"). The geographical distribution of the sea ice cover for each of these different control runs is shown in Hansen et al. (1984). The "alternate old $2 \times CO_2$" experiment produced

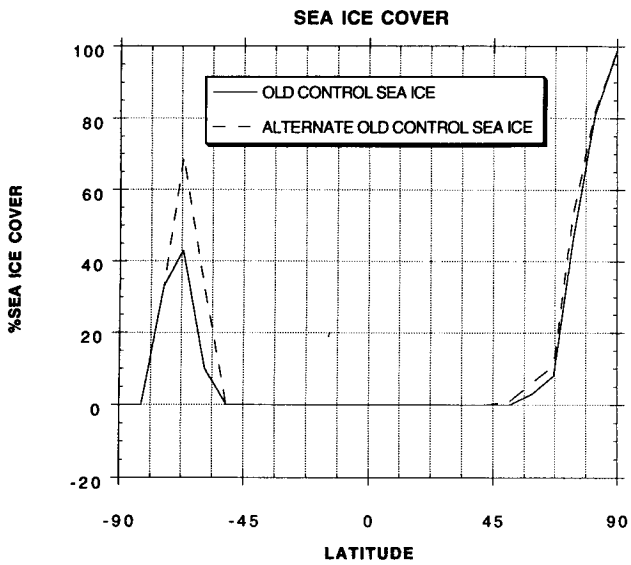

FIG. 1. Annual average sea ice cover in the old control and in the alternate old control runs.

close to a 4.9°C warming, with a relative sea ice reduction of 50% (from 6% absolute to 3%).

The latitudinal distribution of the temperature change due to $2 \times CO_2$ in the two experiments is shown in Fig. 2. The difference in warming is largest at high southern latitudes, where the control run sea ice values were most different and the sea ice changes were largest. The effect diminishes with distance from this region although there is still a substantial response at low latitudes. (As will be discussed in section 3, the sea ice changes induce water vapor and cloud feedbacks that are globally distributed.) For example, in the Tropics the $2 \times CO_2$ water vapor is 36% greater in the "alternate" experiments and 32% in the "old" experiments, while the low-level cloud decrease is 5.1% compared to 3.6%. Shown in Table 1 are the control run sea ice values and their changes due to doubled CO_2 for each hemisphere in the different experiments.

The sea ice difference between the two experiments is greatest in the Southern Hemisphere, consistent with the difference in warming. Apparently the impact of greater Southern Hemisphere sea ice change does not result in high-latitude amplification of the additional warming in the Northern Hemisphere. This result implies that the Southern Hemisphere sea ice change would not be an efficient mechanism for generating ice sheets at high latitudes in the Northern Hemisphere directly via atmospheric/climatic processes. It could provide for interhemispheric influence through mechanisms not included in these experiments, such as alterations in Antarctic bottom water production.

3. The sea ice contribution to warming

What is the sea ice contribution to the simulated warming? As discussed in detail by Ingram et al. (1989), the answer depends on the method of calculation, and in particular on what is meant by "sea ice contribution." If the sea ice contribution is defined as the change (in W m^{-2}) of the radiation imbalance due to altered surface albedo, this definition would seem to isolate the direct sea ice forcing; however, it is not independent of the model's water vapor distribution and, especially, cloud cover, which can shield the surface and minimize the effectiveness of surface albedo changes. If, alternatively, the sea ice contribution is defined as the total response of the system to a change in sea ice, this would encompass the full magnitude of global or local temperature response, of importance for example in the potential growth of ice sheets due to sea ice change. However, this then depends on the sensitivity of the other feedbacks in the modeled system. Below we show the differences between these approaches, and then in subsequent sections concentrate on the practical impacts from changes in sea ice.

a. 1D and 2D analyses

Using a 1D radiative–convective model, Hansen et al. (1984) calculated the radiative effect of the change in surface albedo using the global, annual average output of the "old" and "alternate old" GCM $2 \times CO_2$ experiments and converted the results to global average temperature changes. The impact of global average cloud shielding was included, which substantially reduces the surface albedo effect. Hansen et al. (1984) concluded that the sea ice–snow cover change by itself produced a warming of approximately 0.4°C with the "old control" run procedure and approximately 0.6°C in the "alternate old" run. About 70% of the surface albedo change occurred over nonland areas associated with decreased sea ice.

The sea ice and temperature responses vary strongly both seasonally and geographically. During the South-

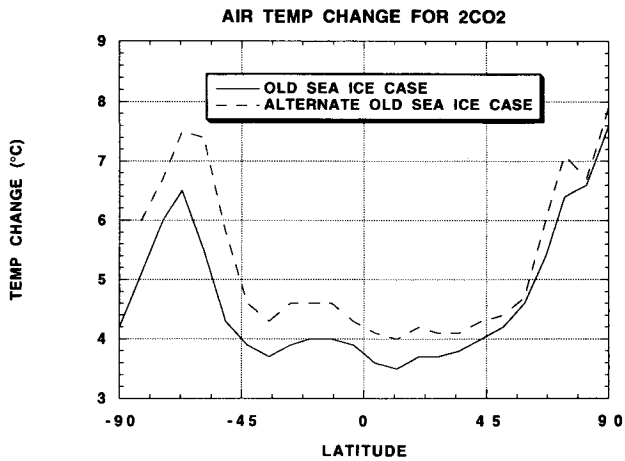

FIG. 2. Annual average surface air temperature change due to $2 \times CO_2$ with the old control and the alternate old control runs.

TABLE 1. Hemispheric sea ice values (%), Control and 2 × CO_2, for the earlier experiments.

	Old control	Old 2 × CO_2	Difference	Alternate old control	Alternate old 2 × CO_2	Difference
Northern Hemisphere	3.92	2.84	−1.08 (−28%)	4.60	3.28	−1.32 (−40%)
Southern Hemisphere	4.26	1.73	−2.53 (−59%)	7.32	2.85	−4.47 (−61%)

ern Hemisphere winter, surface air temperature warming of some 20°C occurs in the regions of sea ice reduction, while in summer the response is just several degrees. The greater sea ice impact on winter surface temperatures is understandable in view of the larger sea ice area in winter. The enhanced impact is in part due to the release of heat from the ocean stored during the summer and in part due to the large stability of the polar atmosphere, which traps added heat at low levels. The summer storage for regions that were previously sea ice covered represents a "time-delayed" form of albedo feedback, since the increased ability to absorb heat in summer is due to the lower surface albedo that results from the sea ice removal. As this effect is associated with the much greater solar insolation available during summer, it is not properly calculated with a 1D annual average analysis, nor is the low-level heat-trapping ability of the winter polar atmosphere, since 1D models normally use a specified lapse rate close to the moist adiabatic.

The limitations of global averaging have been addressed by using a 2D radiative–convective model, including dynamic heat transports between latitudes (Pollack et al. 1993). The surface albedo contribution determined from this analysis in the "old 2 × CO_2" experiment produced a peak temperature response of 2.7°C at 67°S, and a smaller Northern Hemisphere peak of 1.5°C at 74°N. The global average surface albedo effect calculated in this way is approximately 0.3°C. Apparently including the latitudinal distribution, while ignoring the seasonal and geographical effects, does not substantially alter the results.

If one were to take just the atmospheric temperature changes over the regions where sea ice had existed in the control run (hence including seasonal and geographic dependencies), and calculate their contribution to the global average temperature from GCM output, the result again is approximately 0.4°C. This ignores the contribution of the sea ice change to warming elsewhere, and it also assigns all the warming above the sea ice to the sea ice influence itself. Nevertheless, the assessment of the direct sea ice influence of 0.3°–0.4°C in the old 2 × CO_2 experiment, independent of the other feedbacks, appears robust.

What about the total sea ice impact, including sea ice–induced feedbacks in water vapor and cloud cover? The sea ice reduction in the GISS GCM is often associated with increased water vapor (from increased evaporation) and decreased cloud cover (in conjunction with increased atmospheric water-holding capacity and reduced low-level stability) (Rind and Chandler 1991), which would act as positive feedbacks. In the 1D analysis such effects, although they result from the sea ice reduction, are classified as water vapor and cloud feedbacks, since nonlinearities are automatically eliminated by the approach. However, Hansen et al. (1984) used the 1D analysis to explore the nonlinear effects of multiple feedbacks and estimated that the sea ice contribution, including water vapor and cloud effects, was about 1°C in the old 2 × CO_2 experiment and 1.6°C in the alternate old experiment. Dickinson et al. (1987) estimated that about 1.3° of the 3.5°C warming in the 2 × CO_2 experiment of Washington and Meehl (1984) could be attributed to the sea ice–snow cover feedback. Again, uncertainties associated with the annual global-averaging procedure require that the estimates be explored more thoroughly.

b. 3D experiments

In another approach, we can use the difference between the two experiments in which the q flux is incorporated differently into the sea ice. As noted above, the two experiments had different initial sea ice concentrations, and thus different sensitivities. The 35% change in sea ice (from −15% of observed values to +20%) between the two control runs resulted in increased warming of 0.7°C in the doubled CO_2 experiments. Were this to indicate the model sensitivity (in degrees Celsius per percent sea ice change), then since the old 2 × CO_2 experiment experienced a 44% sea ice change via the "heat insertion" approach, it would imply sea ice was responsible for about 0.9°C warming. The result is only approximate because the location of the sea ice differences between the two control runs is not the same as between the control and 2 × CO_2 experiments.

To make this calculation more precise requires an experiment in which the sea ice is not allowed to change in the 2 × CO_2 experiment, while all other feedbacks (and ocean temperatures) are free to vary. Using this approach, Ingram et al. (1989) found that the total sea ice influence amounted to 1°C in the UKMO (U.K. Meteorological Office) 2 × CO_2 run. The experiment is repeated here with the old control run.

The sea ice generated in the GISS "old control run" was saved hourly for one full year for every relevant grid box. These values were then inserted into a 2 × CO_2 run for the corresponding hours, and the model was run to equilibrium. When the sea surface temper-

ature rose above the melting point for sea ice, the model would normally reduce the sea ice, using energy from the water column. However, the sea ice was not allowed to change and energy was conserved by adding the appropriate energy values back to the water. This run is referred to as the "no sea ice change" $2 \times CO_2$ experiment.

The resulting latitudinal warming for the $2 \times CO_2$ experiments with and without sea ice change is shown in Fig. 3. Without allowing for a sea ice response, there is little, if any, high-latitude amplification. The effects are not only felt at high latitudes as tropical warming is reduced as well; tropical water vapor is now only 22% more, while the low-cloud reduction is only 2.2%.

Listed in Table 2 are the relevant changes in the "old $2 \times CO_2$" and in the "no sea ice change $2 \times CO_2$" experiments (the percent changes for clouds, snow cover, sea ice, and albedo are absolute values, while the change in atmospheric water vapor is the percentage change relative to the control run value). Shown in Table 2a are the global values and in Table 2b the values at polar latitudes. The change in surface albedo over the polar regions has been limited when the sea ice remains constant and the planetary albedo at those latitudes actually goes up slightly, associated with an increase in cloud cover. There is still a substantial water vapor increase at high latitudes, since warming the cold air produces a relatively large percentage increase in saturation vapor pressure.

Note that as the sea ice is not constant from year to year in the control run, a 1-yr sampling did not reproduce precisely the 10-yr averages at high latitudes, and the "specified sea ice" was actually 0.6% too small. This should not affect the results in any noticeable way, however, given that the full $2 \times CO_2$ experiment had polar sea ice changes 20 times as large.

The global impact of sea ice on climate sensitivity is shown by the difference between the two experiments; the temperature change between them of 1.56°C is close to four times the contribution from the surface albedo change alone, as estimated above. Hansen et al. (1984) used the results from the "old $2 \times CO_2$" experiment to approximate the various contributions to the equilibrium greenhouse warming, and we can relate the changes in the "no sea ice change" experiment to those values. Doubling atmospheric CO_2 by itself contributes a warming of approximately 1.2°C, the same in both experiments. In the "old $2 \times CO_2$" experiment the water vapor contributed about 1.7°C to the warming. With a somewhat similar profile of change, but a magnitude only 70% as great, the water vapor contribution is (very roughly) approximately 1°C. The changes in surface albedo due to snow cover reductions are only about one-third as large in the no sea ice change experiment, providing warming on the order of 0.1°C. The cloud changes in the "old $2 \times CO_2$" experiment provide warming of 0.9°C; the impact here would be less due to the smaller reduction in low-level-cloud loss, but there would be an additional contribution from the high-cloud gain, which does not occur on the global average in the "old $2 \times CO_2$" experiment (although that experiment does have an increase in average cloud altitude due to the decrease in low-level clouds). Overall, the planetary albedo change in the "no sea ice change" experiment is some 40% that of the "old $2 \times CO_2$" experiment; thus, the impact of the change in cloud cover plus surface albedo would be 40% of the 0.8°C warming estimated by Hansen et al. due to these effects, or 0.3°C. This leaves a small additional contribution due to cloud cover altitude changes to produce the calculated warming of 2.6°C.

TABLE 2. Annual changes due to $2 \times CO_2$.

(a) Global averages

Parameter	Old experiment	No sea ice change
Surface temperature	+4.17°C	+2.61°C
Planetary albedo	−1.9%	−0.8%
Low-level clouds	−2.3%	−1.4%
High-level clouds	−0.3%	+0.8%
Atmospheric water vapor	+32.4%	+21.6%
Surface albedo	−0.9%	−0.3%
Sea ice cover	−1.8%	0%
Snow cover	−2.9%	−0.6%

(b) Polar (55°–90°N, 55°–90°S) averages

Parameter	Old experiment	No sea ice change
Surface temperature	5.6°C	2.67°C
Planetary albedo	−1.7%	0.1%
Low-level clouds	0.1%	0.2%
High-level clouds	0.4%	0.1%
Atmospheric water vapor	42.5%	25.0%
Surface albedo	−7.5%	−0.8%
Sea ice cover	−9.8%	−0.6%
Snow cover	−12.0%	−2.2%

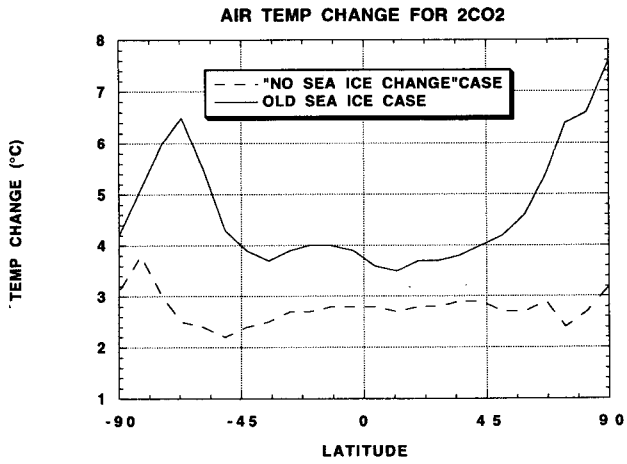

FIG. 3. Annual average surface air temperature change due to $2 \times CO_2$ in the old control run and in the no sea ice change experiment.

Thus, the reduced sensitivity when no sea ice is allowed to change is primarily due to reductions in the positive feedbacks of water vapor and cloud cover changes. In the tropical regions, where sea ice albedo effects are nonexistent, these variables are responsible for the total radiative effect (their percentage change in the Tropics was given above in conjunction with the discussion of Fig. 3).

Note that the magnitude of the global, annual average sea ice contribution, 1.56°C, is somewhat higher than the 1°C value estimated by Hansen et al. (1984) or Ingram et al. (1991). The Hansen et al. values were derived from 1D, annual average considerations from which the nonlinear effects of combined processes were estimated. It is not surprising that the nonlinear impact of sea ice perturbations, whose distribution is high-latitude specific, would not be perfectly well represented in a global-average analysis; differences in the absolute magnitude of the various responses between high latitudes and the global average are evident in Tables 2a and 2b. As discussed by Ingram et al. (1989), the radiative emissions associated with cloud cover, water vapor, and temperature variations at individual locations cannot be duplicated completely accurate by globally averaging these parameters; in the UKMO 2 $\times$ CO_2 run, the 1D procedure overestimates the GCM warming by some 20%. Furthermore, even without these problems, the authors also note that the lack of the seasonal storage effect would lead to slightly smaller warming in the 1D model. This is especially true when considering sea ice, whose loss allows heat to be gained by the ocean in summer from incoming solar insolation, and preferentially given back to the atmosphere during winter when the low-level stability is at its greatest, and its effect on the surface air temperature is therefore largest.

Ingram et al. (1989) define a feedback parameter,

$$\lambda = \Delta Q \,(\text{from } 2 \times CO_2)/\Delta T. \qquad (3)$$

In their experiments with and without sea ice variations, the warming amounted to 5.2°C and 4.2°C, respectively. Therefore, with a 4 W m^{-2} initial tropopause imbalance due to 2 $\times$ CO_2, λ = 0.77, and 0.95 W m^{-2} K^{-1}, respectively, in these two experiments, and their 1°C influence of sea ice was associated with a feedback parameter $\lambda_{\text{sea ice}}$ = 0.18 W m^{-2} K^{-1}. In the GISS model, the values of λ are 0.95 and 1.51 W m^{-2} K^{-1} with and without sea ice variations, so that $\lambda_{\text{sea ice}}$ = 0.56 W m^{-2} K^{-1}.

With the UKMO model, Ingram et al. (1989) found that by specifying the sea ice equally in the control and doubled CO_2 runs, doubling atmospheric CO_2 led to a surface albedo reduction of 0.24% (absolute) compared to the control run, as opposed to a reduction of 0.59% in the full 2 $\times$ CO_2 simulation, for a difference of 0.35%. With the GISS model, the surface albedo reduction was 0.3% with "no sea ice change" (Table 2a), a 0.6% smaller reduction than in the "old 2 $\times$ CO_2" experiment. The larger albedo difference in the GISS model approximately accounts for the somewhat greater contribution from sea ice to its sensitivity. The surface albedo impact of sea ice depends upon where the sea ice was in the control run, its thickness (including the grid resolution), the model specifications for sea ice and snow albedos, and the cloud cover over the sea ice or open ocean. All of these values may vary between models. Although Ingram et al. (1989) comment that the UKMO model and the GISS model probably have similar sea ice extents, albedos, and high-latitude cloud cover, the sensitivities of the models obviously differ when it comes to sea ice perturbations.

In addition to the control run specifications, the results also depend on the other sensitivities in the system. For example, the cloud cover sensitivity could well be different; J. Hansen (1994, personal communication) has recently run experiments with a sector model version of the GISS GCM and found that the sea ice influence was substantially reduced in a 2% solar irradiance reduction experiment when cloud cover was kept fixed (the effect did not arise in a 2% solar increase experiment). With varying methods of calculating the sea ice impact, Ingram et al. (1989) note that $\lambda_{\text{sea ice}}$ values range from 0.16 to 0.7 in doubled CO_2 experiments of different models; the GISS 1D analysis of the full impact of sea ice gave values of 0.28 and 0.37 in the "old" and "alternate old 2 $\times$ CO_2" experiments compared to the 3D calculated value of 0.56 in the old experiment.

These results use the sea ice distribution and thickness calculated from the "old" GCM runs. In the next section, we describe an improved sea ice dataset for ice concentrations and thicknesses.

4. Revised sea ice concentrations and thickness

Revised sea ice concentrations were derived from monthly averaged satellite passive-microwave data for the year 1986. They were digitized from polar stereographic maps of sea ice concentrations and converted to the latitude–longitude grid of the GISS model.

The satellite data are from the *Nimbus-7* Scanning Multichannel Microwave Radiometer (SMMR). This instrument transmitted high quality data on an every-other-day basis throughout 1986, and, in fact, for almost the entire period from the launch of the *Nimbus-7* in late October 1978 through the turning off of the scanning mechanism on the SMMR in mid-August 1987. The SMMR had 10 channels, receiving horizontally and vertically polarized radiation at each of five microwave wavelengths. Its usefulness for sea ice studies derives from the sharp contrast between the microwave emissions of sea ice and sea water, and the limited amount of atmospheric interference with microwave radiation.

The algorithm used to convert from the SMMR radiative data to sea ice concentrations makes use of three

of the SMMR channels and two ratios, a polarization ratio and a gradient ratio, calculated from them. The three channels are for horizontally polarized radiation at a wavelength of 1.7 cm and vertically polarized radiation at wavelengths of 1.7 and 0.81 cm, and the ratios are for the polarization between the two 1.7-cm channels and the gradient between the two vertically polarized channels. The use of ratios reduces the spurious effects that temperature variations can have on the ice-concentration calculations. The polarization ratio is significantly greater for water than for ice, whereas the gradient ratio helps to distinguish two major types of sea ice, ice that has undergone a summer melt season (often termed multiyear ice) and ice that has not (often termed first-year ice). Together, the contrasts allow the primary calculation of ice concentrations and the secondary calculation of the concentrations of the two separate ice types. A detailed description of the algorithm is provided in Gloersen et al. (1992). The calculated sea ice concentrations are estimated to have an accuracy of ±7%. Their spatial resolution is approximately 55 km, the same as the resolution of the 1.7-cm data (Gloersen et al. 1992).

The combination of the SMMR characteristics and the 955-km *Nimbus-7* orbit allowed data coverage by the SMMR everywhere equatorward of about 84.6° latitude. This meant that in the Southern Hemisphere, where the Antarctic continent fully covers the 84.6°–90°S latitude range, no ocean area was without data coverage. In the Northern Hemisphere, however, the 84.6°–90°N region of the central Arctic Ocean had no calculated sea ice concentrations from the SMMR data. We have assumed 100% ice concentrations in this region, with an error probably of no greater than 4%.

The SMMR-derived sea ice concentrations for the full 1978–1987 period of the SMMR data have been compiled and analyzed in an atlas by Gloersen et al. (1992) and have been used extensively in a variety of sea ice studies. Further information on the algorithm, the error analysis, the revealed regional, seasonal and interannual variability in the sea ice covers of both the Arctic and the Antarctic, and the prior studies with the SMMR data can all be found in the Gloersen et al. book. Color-coded January and July images for both hemispheres are presented in Fig. 4. The digital data, gridded to grid elements of approximately 25 km × 25 km, can be obtained on CD-ROMs from the National Snow and Ice Data Center in Boulder, Colorado.

No datasets for sea ice thickness exist comparable to the ice concentration datasets from the SMMR. Ice thicknesses are not yet obtainable from satellite data and have been measured only sporadically by field trips on the ice and, for the Arctic, some submarine tracks under the ice, as analyzed, for instance, by McLaren (1989) and Wadhams (1990). Bourke and Garrett (1987) have compiled the available ice thickness data for the Arctic and have produced seasonal contour maps of ice thickness, indicating climatic-type-averaged conditions, not specified for an individual year. It is these maps that we have taken, digitized to the latitude–longitude grid of the GISS model, and interpolated to the individual months. Thicknesses throughout the year tend to be greatest north of Greenland and the eastern Canadian Archipelago, as the ice is compacted against the coastline due to the general ocean and atmospheric circulation in the region. Thicknesses in this region are generally in the range of 4–7 m, in comparison to the 3–5-m thicknesses at the pole itself and the 0–2-m thicknesses along the Siberian coast (Bourke and Garrett 1987).

In the case of the Antarctic, the available ice thickness observations are so few that we have simply set thicknesses at the outer edge of the pack (determined from the satellite data) to 50 cm and thicknesses poleward of the outer edge to 1–1.5 m, dependent on the distance to the outer edge. These are essentially smoothed fields in approximate agreement with the limited reported observations [e.g., Ackley (1979) in the Weddell Sea; Streten and Pike (1984) in the Indian Ocean sector of the Southern Ocean; Allison (1989) off East Antarctica; Lange and Eicken (1991) in the northwestern Weddell Sea], although details vary. In the Weddell Sea in particular, Ackley (1979) reported thicker ice, of about 3-m thickness, near the edge of the ice pack off the northeast coast of the Antarctic Peninsula where multiyear ice often drifts due to the generally cyclonic circulations in the Weddell Sea region.

5. 2 × CO_2 experiments with revised sea ice

The new control sea ice distributions and thicknesses presented in section 4 were input to the GCM, and the ocean heat convergences necessary to reproduce them were calculated (with the "heat insertion from the bottom and sides" approach). Then the model was run with those new convergences with both current and doubled atmospheric CO_2. These experiments are referred to as the "new control" and "new 2 × CO_2" experiments, respectively. The zonal distribution of the percent sea ice cover from the "old control" and the "new control" runs are shown in Fig. 5a. The zonal distributions from the two control runs are quite similar, although the old control run underestimated the distributions given by Alexander and Mobley (1974) in the Southern Hemisphere, due to the difficulty in using the q flux. The "new control" run successfully reproduces the satellite data. Therefore, the satellite sea ice cover is less than the older observations specified, especially in the Southern Hemisphere. The older observations produced a sea ice cover of 4.2% in the Northern Hemisphere, 5.4% in the Southern Hemisphere, and 4.8% globally. The satellite data give 3.9% in the Northern Hemisphere, 3.4% in the Southern Hemisphere, and 3.6% globally. As the "old control" run actually used a sea ice cover that is closer to the

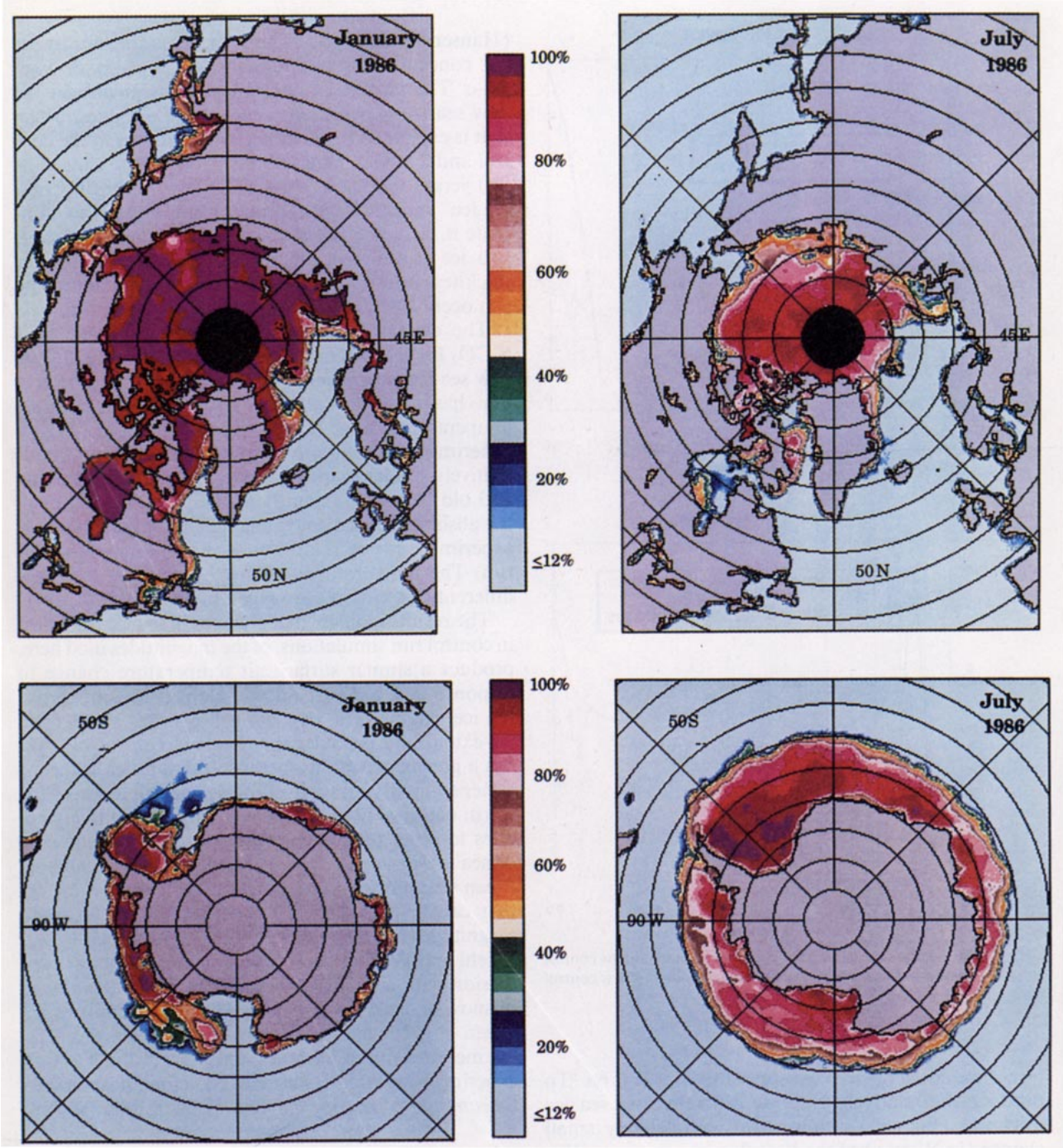

FIG. 4. Monthly average sea ice concentrations for January and July for both the (a) north and (b) south polar regions. Ice concentrations are derived from the radiative data of the *Nimbus-7* SMMR and were digitized to the GISS model grid for use in the model simulations.

satellite values than the "alternate old control" run, it is probably more realistic in that respect. The ability of the different control runs to duplicate the respective observations is evident by comparing these observed values with the control run values shown in Tables 1 and 3.

In contrast to the percent sea ice cover, the sea ice thicknesses are now much smaller (Fig. 5b). The "old control" run values were too thick in the Antarctic region, resulting from a combination of the greater thickness originally specified in the model version used to calculate ocean heat convergences and the difficulty in reproducing sea ice thickness with the heat convergences.

This latter point is emphasized by the difference in ocean heat convergences associated with the two sea ice control runs. The zonal averages of the respective

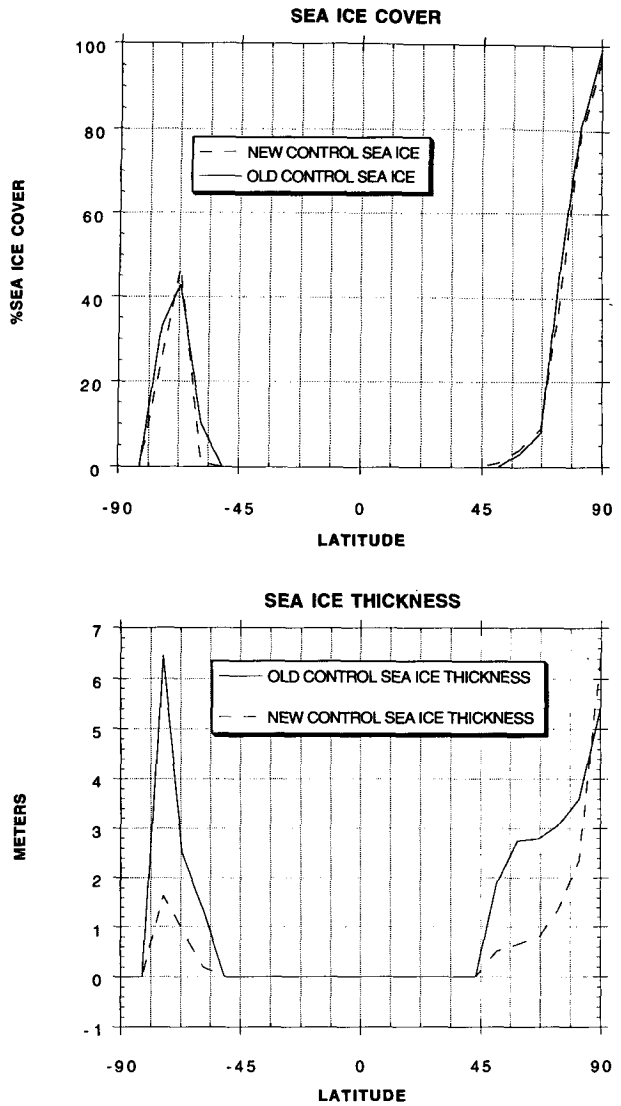

FIG. 5. (a) Annual average sea ice cover in the old and new control runs. (b) Annual average sea ice thickness in the old and new control runs.

heat flux convergences are presented in Fig. 6a. To produce the relatively extreme differences in sea ice thickness (Fig. 5b) requires only a relatively small change (in W m^{-2}) of the heat flux convergence (Fig. 6a). The calculated ocean heat transports to produce these convergences are given in Fig. 6b. While significant differences arise poleward of 45°S, overall the increase in global poleward heat transport associated with the thinner sea ice is 9.5%. Conversely, this indicates that a change in poleward heat transport of this magnitude and distribution can produce the large changes in sea ice thickness of Fig. 5b in the GISS model.

The "new control" run was then used for a 2 × CO_2 experiment similar to that of the "old control" run (Hansen et al. 1984). The respective changes in sea ice concentration and thickness are given in Figs. 7a–c. The change in concentration is greater in the new sea ice experiments than in the old ones, a fact that is explained by the relative thicknesses in the control and 2 × CO_2 experiments in the "old" runs (Fig. 7b) versus the "new" runs (Fig. 7c). Since the "new sea ice" run starts with thinner ice, it is easier to eliminate it, reducing the concentrations. Therefore, these two ice parameters are related; control run sea ice thickness influences the change in concentration that can occur.

The change in surface air temperature due to 2 × CO_2 for the two experiments is given in Fig. 8. The new sea ice experiment, with its greater sea ice reduction, has increased warming everywhere. This resulting temperature change between the new and old 2 × CO_2 experiments is qualitatively and, coincidentally, quantitatively similar to the difference between the alternate and old 2 × CO_2 experiments (Fig. 2), even though the absolute sea ice cover change in the new 2 × CO_2 experiment is not as large as in the alternate 2 × CO_2 run. The temperature and sea ice changes for these different experiments are given in Table 3.

The results indicate that changes in sea ice thickness in control run simulations, of the magnitudes used here, produce a similar surface air temperature change in response to 2 × CO_2 as do differences in control run sea ice extents. The new control run has smaller sea ice extent and is colder than the old control run, yet has a greater sensitivity because the thinner sea ice is easier to totally remove, allowing the influence of the warm ocean to be fully felt. The same result likely applies to other parameters that can influence the ease of sea ice disappearance, such as the sea ice albedo, ocean heat transports, and cloud cover response, factors that can help explain the range of sea ice feedback magnitudes found in other studies (Ingram et al. 1989). Meehl and Washington (1990) reached a similar conclusion with a GCM experiment in which the albedo of snow and sea ice was reduced for temperatures between −10°C and 0°C; the control run was 1°C warmer and its sea ice less extensive, yet the 2 × CO_2 experiment was 0.5°C warmer. Therefore, it is not only the *amount* of sea ice capable of being removed (or

TABLE 3. Global annual average temperatures and sea ice covers.

Experiment	Temperature (°C)	Sea ice (%)
Old 2 × CO_2	18.44	2.28
Old control	14.27	4.09
Difference	4.17	−1.81
Alternate 2 × CO_2	17.98	3.07
Alternate old control	13.20	5.96
Difference	4.78	−2.89
New 2 × CO_2	17.89	1.30
New control	13.11	3.70
Difference	4.78	−2.40

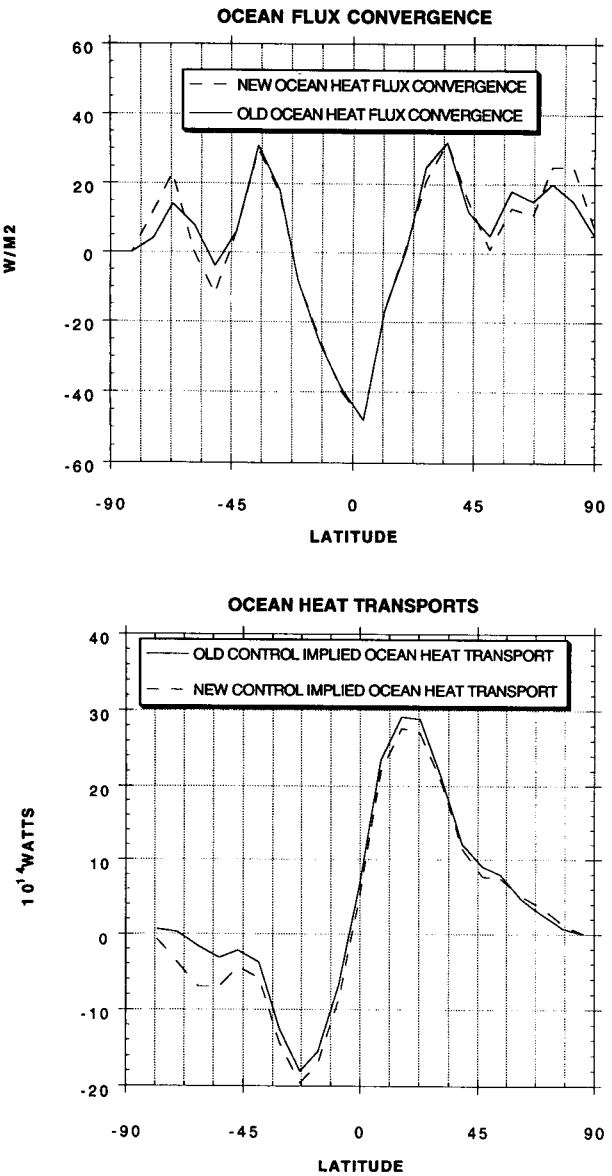

FIG. 6. (a) Annual average specified ocean heat flux convergence in the old and new control runs. (b) Annual average implied ocean heat transports in the old and new control runs.

added), it is also the *ease* with which this can occur, an ease that is increased in warming experiments when the control run values are thinner (or sea ice albedo is less).

6. Discussion

There are several reasons for the interest in sea ice sensitivity to atmospheric climate change, the most obvious being the feedback effect of sea ice on the atmosphere and on the overall climate sensitivity. In addition, if sea ice changes substantially when the atmosphere is perturbed, its effect on high-latitude oceans, because of its high albedo and strong insulating properties as well as the salt rejection during ice formation and aging, may be to alter deep-water formation. Numerous observations imply that North Atlantic Deep Water production has decreased in colder climates, but the sea ice contribution to this phenomenon is yet to be resolved.

Another important reason for the interest in sea ice sensitivity is that, on a local scale, changes in sea ice can impact the moisture budget for ice sheets and, therefore, potential sea level variations. For example, large sea ice reductions around Antarctica would be expected to increase evaporation from the ocean, which would increase the moisture content of the air and allow for greater moisture to fall as snow over the land, sequestering water and thereby reducing sea level. To investigate the sensitivity of this mechanism to the different sea ice responses, we calculate the net water mass budget for Antarctica in the different $2 \times CO_2$ experiments.

The results are presented in Table 4. For each quantity, the top line shows the value from the respective control run, the second line the value for the doubled CO_2 experiment, and the third line the change due to the warmer climate. The alternate and new sea ice runs show a greater warming than the standard experiment, and the new sea ice run has the largest warming at lower latitudes (74°S), which helps produce the largest runoff change. All runs with sea ice reductions show a tendency for negative mass balance over Antarctica at 74°S and positive mass balance at the pole relative to the control run, but the magnitudes differ in conjunction with the differing temperature, precipitation, and runoff changes among the experiments.

As shown in the last line of the table, the hydrologic changes over Antarctica in the new sea ice run would contribute a sea level increase of 0.23 cm yr^{-1} (relative to its control run). [This value is within the range of estimated sea level rise due to thermal expansion at the time of equivalent CO_2 doubling (Houghton et al. 1992).] The standard run produces a sea level increase of 0.13 cm yr^{-1}, and the alternate run gives a sea level increase of only 0.003 cm yr^{-1}. In the experiment in which sea ice is not allowed to change, a small sea level increase would occur, for while the runoff due to melting is reduced compared with the other $2 \times CO_2$ runs, so is the precipitation increase. In none of these experiments does a mass balance increase occur over Antarctica. There are many physical land–ice processes that have not been properly included, such as calving, and the runoff would not necessarily remove mass until crevices were saturated. Hence, these results are not predictive of sea level changes and only serve to emphasize that the simulated mass balance over ice sheets is sensitive to the sea ice distribution and thickness in the control runs.

The global effects of sea ice change are associated with its contribution to the overall climate sensitivity.

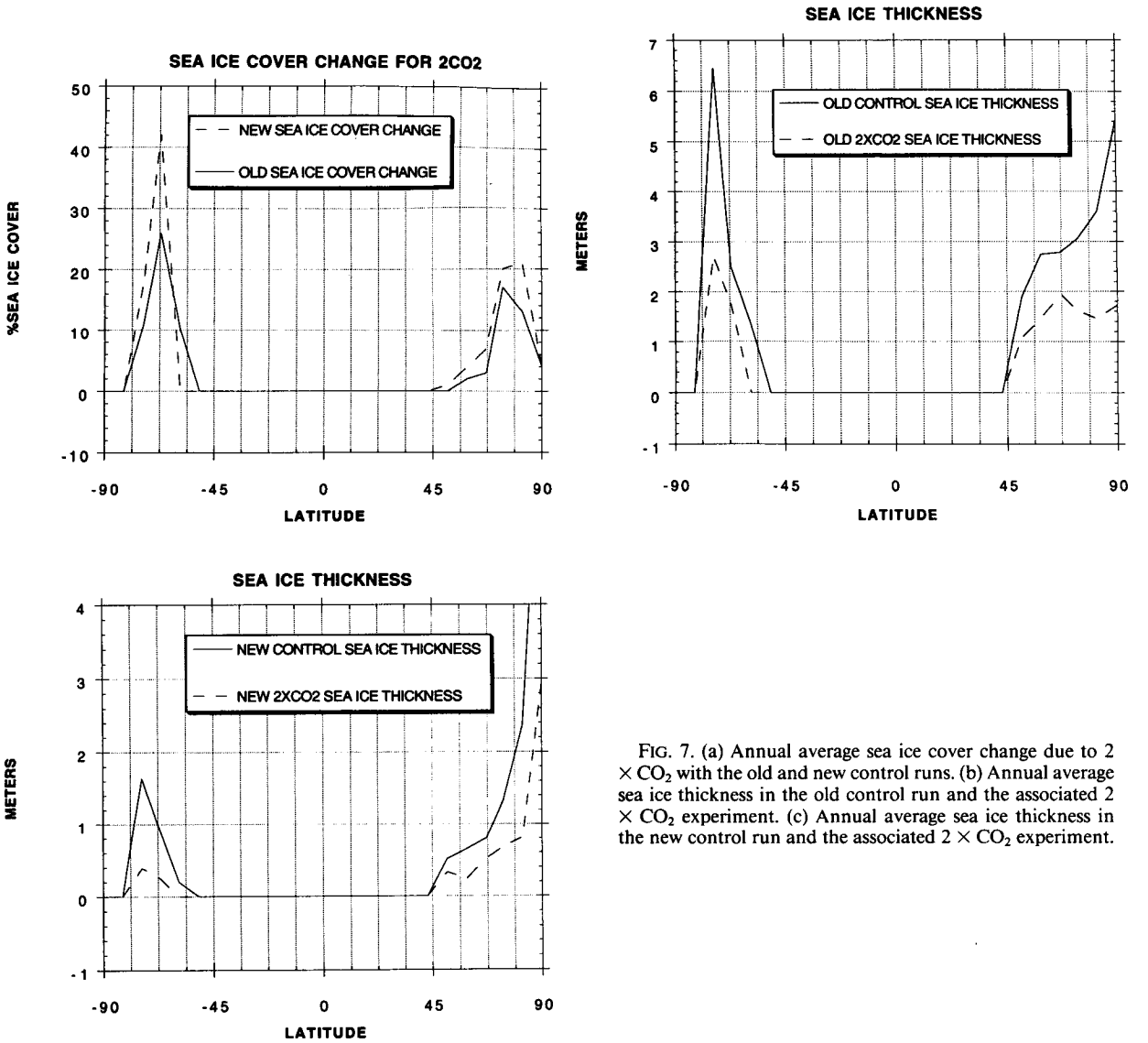

FIG. 7. (a) Annual average sea ice cover change due to 2 $\times$ CO_2 with the old and new control runs. (b) Annual average sea ice thickness in the old control run and the associated 2 $\times$ CO_2 experiment. (c) Annual average sea ice thickness in the new control run and the associated 2 $\times$ CO_2 experiment.

As discussed by Ingram et al. (1989) and reemphasized here, the full sea ice impact, due to its nonglobal extent and seasonal variation, is much more difficult to analyze in lower-dimensional models using GCM output than when evaluated with the 3D GCM directly. The global, annual average results from the experiment in which sea ice is not allowed to change indicates that the sea ice response, when allowed to initiate the other feedbacks in the model (primarily water vapor and cloud cover changes), accounts for about 37% of the atmospheric temperature sensitivity to 2 $\times$ CO_2 in the GISS model, similar to the value estimated for the National Center for Atmospheric Research model (Dickinson et al. 1987) and about double the percentage of the UKMO model (Ingram et al. 1989).

We have concentrated in this paper on the contribution of sea ice in GCMs to climate sensitivity when the climate is being warmed. The sea ice contribution to the surface temperature response is actually larger, in absolute terms, in experiments when the climate is cooled. Pollack et al. (1993) discuss two such experiments, one in which the solar radiation is reduced by 2% through the inclusion of volcanic aerosols, and the other using the CLIMAP- (1981) prescribed ice age boundary conditions.

With the equivalent 2% solar irradiance reduction due to volcanic aerosols, the GISS model produces a cooling of 5.4°C (Rind et al. 1992; Pollack et al. 1993). The sea ice cover in this experiment increased by 100% (150% in the Southern Hemisphere). Its *direct* contribution to the resulting surface air temperature change (along with the snow cover increase) as evaluated with a 2D radiative–convective model amounted to approximately 0.8°C, or close to 15% of the calculated

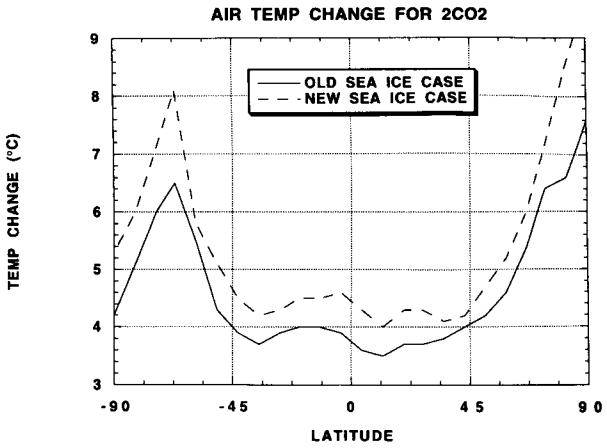

FIG. 8. Annual average surface air temperature change due to $2 \times CO_2$ in the old and new experiments.

cooling. In the ice age experiment, with a global cooling of 3.6°C, the CLIMAP-specified sea ice was increased by 85%. Its direct contribution to the global cooling, along with the calculated snow cover change, amounted to 0.7°C (Hansen et al. 1984) or about 20%. Compare these percentages to the approximate 10% contribution, as calculated by 1D analysis, of the direct surface albedo impact in warming experiments [$2 \times CO_2$ and +2% solar irradiance (Hansen et al. 1984)].

With an actual 2% reduction in solar irradiance, the GISS "old control" run cools by 5.8°C (Rind and Overpeck 1994). When this experiment was rerun with "no sea ice change," the cooling was reduced to 3.56°C. Thus, the total sea ice impact amounted to 39% of the resultant cooling or 2.26°C, compared to 37% in the $2 \times CO_2$ warming experiment or 1.56°C. With a 2% increase in solar irradiance the warming is 4.0°C (Hansen et al. 1984). The greater total effect of sea ice in the cooling experiment therefore accounts for at least part of the difference between the solar increase and decrease results. It is associated with the greater geographical area available for sea ice expansion as opposed to contraction, with the region of expansion impacting areas (lower latitudes) of greater sunshine. Despite this importance of sea ice for colder climates, the "alternate" and "old" $2 \times CO_2$ experiments indicated that changes in Southern Hemisphere sea ice did not lead to increased amplification of climate change at high northern latitudes, which would be necessary for ice-sheet growth and ice age initiation, at least without inducing changes in ocean circulation not included in these experiments.

In this paper, we have used more realistic sea ice thicknesses in the control run than were previously used and found an increased sensitivity to climate change. The thinner ice was easier to remove entirely, allowing a maximum surface albedo response and amplifying the warming by about 15% (from 4.17° to 4.78°C). This result indicates that sea ice thickness is a relevant parameter to consider when comparing model sensitivities, especially if the differences are as large as those considered here. It also illustrates that it is not only the amount of sea ice in the control run that is important for modeled climate sensitivity, it is also the ease with which the sea ice can be removed, which depends upon many parameterizations.

This last point emphasizes that the actual contribution of sea ice to climate sensitivity can only be ascertained with realistic physical parameterizations, especially for sea ice and ocean processes. The sea ice

TABLE 4. $2 \times CO_2$ results over Antarctica.

Parameter	Old runs	Alternate old runs	New runs	No sea ice change
Surface temperature (°C)				
Control	−32.7	−34.3	−33.3	−32.7
$2 \times CO_2$	−27.5	−28.3	−27.2	−28.9
Δ	5.2	6.0	6.1	−3.8
Precipitation (mm d^{-1})				
Control	0.92	0.81	0.87	0.92
$2 \times CO_2$	1.27	1.22	1.22	1.17
Δ	0.35	0.41	0.35	0.25
Evaporation (mm d^{-1})				
Control	0.15	0.15	0.15	0.15
$2 \times CO_2$	0.20	0.20	0.19	0.20
Δ	0.05	0.05	0.04	0.05
Runoff (mm d^{-1})				
Control	0.11	0.05	0.15	0.11
$2 \times CO_2$	0.51	0.41	0.63	0.35
Δ	0.40	0.36	0.48	0.24
Net ice accumulation (mm d^{-1})				
Control	0.66	0.61	0.57	0.66
$2 \times CO_2$	0.56	0.61	0.40	0.62
Δ	−0.10	0	−0.17	−0.04
Sea level change (cm yr^{-1})	0.13	0	0.23	0.05

and ocean transport schemes used in these experiments are extremely simple. There are good reasons to believe that models of this nature underestimate negative feedbacks that may arise, especially on short timescales, in the Southern Ocean due to vertical mixing with the warm waters below (Martinson 1993). Inclusion of a more realistic sea ice model and then a more realistic ocean model are the subjects of ongoing work.

7. Conclusions

Following are the main conclusions of this study:

1) Alternative applications of the q flux incorporation to sea ice strongly impact the Southern Hemisphere sea ice values in the GISS model control runs and their changes in $2 \times CO_2$ experiments. The results strongly influence the Southern Hemisphere high-latitude surface air temperature response to increased CO_2 (greater control run sea ice, greater climate sensitivity). A significant impact also occurs at low latitudes due to water vapor and cloud feedbacks. Effects of these Southern Hemisphere sea ice changes are of much less importance at high northern latitudes, of relevance to the question of ice age initiation.

2) Comparisons to the satellite data indicate that the sea ice coverage in the "old" GCM experiment was closer to observations than in the "alternate old" run where sea ice was too extensive, and thus the "old 2 $\times CO_2$" warming (of 4.2°C) is more appropriate in this respect than the "alternate old" value (of 4.8°C) [however, see (4) below].

3) The direct sea ice–snow cover impact on global, annual average surface temperature response to 2 $\times CO_2$ is approximately 0.4°C in the old runs as estimated with 1D and 2D models; however, when considering the total sea ice effects as determined by a 3D model experiment in which sea ice is not allowed to change, the contribution rises to 1.56°C (for a sea ice feedback parameter $\lambda_{\text{sea ice}} = 0.56$). The direct effect thus amounts to about 10% of the surface air temperature change, while the total effect is approximately 37%.

4) With more realistic (smaller) sea ice thicknesses in the control run, the model's temperature sensitivity to $2 \times CO_2$ increases by about 15% (to 4.8°C). This result emphasizes that it is not only the extent of control run sea ice that influences model climate sensitivity, it is also the ease with which the ice can be removed, both contributing in the same sense of greater sea ice removal, greater climate sensitivity. Changes of this magnitude in climate sensitivity can be produced in this model by variations of 10% in global poleward ocean heat transports.

5) The sea ice changes in the different $2 \times CO_2$ experiments affect the ice mass balance over Antarctica, implying global sea level changes due to this effect alone, ranging from increases of 0.23 cm yr^{-1} to no change. While the actual Antarctic land–ice mass balance will also be affected by processes not included in these assessments, the results illustrate the importance of sea ice changes to Antarctic thermal and ice mass budgets.

6) All of the above results emphasize the necessity for realistic sea ice and ocean models/parameterizations for the proper determination of climate sensitivity and future climate impacts.

Acknowledgments. This work was supported directly by NASA Polar Programs Grant NAGW 1844 and indirectly by the NASA Climate Modeling Program that funds climate model development at GISS. RH was partly supported by NSF Grant ATM9006307. The LDEO contribution number is 5300.

REFERENCES

Ackley, S. F., 1979: Mass-balance aspects of Weddell Sea pack ice. *J. Glaciol.*, **24,** 391–405.

Alexander, R. C., and R. L. Mobley, 1974: Monthly average sea-surface temperatures and ice-pack limits on a 1° global grid. Rep. 4-1310-ARPA, Rand Corp., Santa Monica, CA, 30 pp.

Allison, I., 1989: The East Antarctic sea ice zone: Ice characteristics and drift. *GeoJournal,* **18,** 103–115.

Bourke, R. H., and R. P. Garrett, 1987: Sea ice thickness distribution in the Arctic Ocean. *Cold Reg. Sci. Technol.,* **13,** 259–280.

Cess, R. D., and Coauthors, 1991: Interpretation of snow-climate feedback as produced by 17 general circulation models. *Science,* **253,** 888–892.

CLIMAP Project Members, 1981: Seasonal reconstruction of the earth's surface at the last glacial maximum. *Geol. Soc. Amer.,* Map and Chart Series, No-36.

Dickinson, R. E., G. A. Meehl, and W. M. Washington, 1987: Ice-albedo feedback in a CO_2 doubling simulation. *Clim. Change,* **10,** 241–248.

Gloersen, P., W. J. Campbell, D. J. Cavalieri, J. C. Comiso, C. L. Parkinson, and H. J. Zwally, 1992: Arctic and Antarctic Sea Ice, 1978–1987: Satellite Passive-Microwave Observations and Analysis. NASA SP-511, National Aeronautics and Space Administration, Washington, DC, 290 pp.

Hansen, J. E., G. Russell, D. Rind, P. Stone, A. Lacis, S. Lebedeff, R. Rudey, and L. Travis, 1983: Efficient three-dimensional global models for climate studies: Models I and II. *Mon. Wea. Rev.,* **111,** 609–662.

——, and Coauthors, 1984: Climate sensitivity: Analysis of feedback mechanisms. Climate Processes and Climate Sensitivity, *Geophys. Monogr.,* No. 29, Amer. Geophys. Union, Washington, DC.

Houghton, J. T., B. A. Callander, and S. K. Varney, Eds., 1992: *Climate Change 1992.* Cambridge University Press, 93 pp.

Imbrie, J., and Coauthors, 1992: On the structure and origin of major glaciation cycles. *Paleoceanography,* **7,** 701–738.

Ingram, W. J., Wilson, C. A., and J. F. B. Mitchell, 1989: Modeling climate change: An assessment of sea ice and surface albedo feedbacks. *J. Geophys. Res.,* **94,** 8609–8622.

Lange, M. A., and H. Eicken, 1991: The sea ice thickness distribution in the northwestern Weddell Sea. *J. Geophys. Res.,* **96,** 4821–4837.

Martinson, D., 1993: Ocean heat and seasonal sea ice thickness in the southern ocean. *Ice in the Climate System,* W. Peltier, Ed. NATO ASI Series, Vol. I, Springer-Verlag, 597–609.

McLaren, A. S., 1989: The under-ice thickness distribution of the Arctic Basin as recorded in 1958 and 1970. *J. Geophys. Res.,* **94,** 4971–4983.

Meehl, G. A., and W. M. Washington, 1990: CO_2 climate sensitivity and snow-sea-ice albedo parameterization in an atmospheric GCM coupled to a mixed-layer ocean model. *Clim. Change,* **16,** 283–306.

Miller, G. H., and A. de Vernal, 1992: Will greenhouse warming lead to Northern Hemisphere ice-sheet growth? *Nature,* **355,** 244–246.

Morgan, V. I., I. D. Goodwin, D. M. Etheridge, and C. W. Wookey, 1991: Evidence from Antarctic ice cores for recent increases in snow accumulation. *Nature,* **354,** 58–60.

Orvig, S., 1970: *Climates of the Polar Regions.* Elsevier, 370 pp.

Parkinson, C. L., J. C. Comiso, H. J. Zwally, D. J. Cavalieri, P. Gloersen, and W. J. Campbell, 1987: Arctic Sea Ice, 1973–1976: Satellite Passive-Microwave Observations. NASA SP-489, National Aeronautics and Space Administration, Washington, DC, 296 pp.

Peel, D. A., 1992: Ice core evidence from the Antarctic Peninsula region. *Climate Since A.D. 1500,* R. S. Bradley and P. D. Jones, Eds., Routledge, 679 pp.

Pollack, J. B., D. Rind, A. Lacis, J. E. Hansen, M. Sato, and R. Ruedy, 1993: GCM simulations of volcanic aerosol forcing. Part I: Climate changes induced by steady state perturbations. *J. Climate,* **6,** 1719–1742.

Rind, D., and M. Chandler, 1991: Increased ocean heat transports and warmer climate. *J. Geophys. Res.,* **96,** 7437–7461.

——, and J. Overpeck, 1994: Hypothesized causes of modeled decade to century scale variability. *Quat. Sci. Rev.,* **12,** 357–374.

——, N. K. Balachandran, and R. Suozzo, 1992: Climate change and the middle atmosphere. Part II: The impact of volcanic aerosols. *J. Climate,* **5,** 189–208.

Robinson, D. A., F. T. Kemig, and K. F. Dewey, 1990: Recent variations in Northern Hemisphere snow cover. *Proc. 15th NOAA Annual Climate Diagnostics Workshop,* Asheville, NC, NOAA, 219–224.

Spelman, M. J., and S. Manabe, 1984: Influence of oceanic heat transport upon the sensitivity of a model climate. *J. Geophys. Res.,* **89,** 571–586.

Streten, N. A., and D. J. Pike, 1984: Some observations of the sea-ice in the southwest Indian Ocean. *Aust. Meteor. Mag.,* **32,** 195–206.

Wadhams, P., 1990: Evidence for thinning of the Arctic ice cover north of Greenland. *Nature,* **345,** 795–797.

Walsh, J., and C. Johnson, 1979: An analysis of Arctic sea ice fluctuations. *J. Phys. Oceanogr.,* **9,** 580–591.

Washington, W. M., and G. A. Meehl, 1984: Seasonal cycle experiment due to a doubling of CO_2 with an atmospheric general circulation model coupled to a simple mixed-layer ocean model. *J. Geophys. Res.,* **89,** 9475–9503.

Zwally, H. J., J. C. Comiso, C. L. Parkinson, W. J. Campbell, F. D. Carsey, and P. Gloersen, 1983: Antarctic Sea Ice, 1973–1976: Satellite Passive-Microwave Observations. NASA SP-459, National Aeronautics and Space Administration, Washington, DC, 206 pp.